

Continuity of currents across neighboring cells in PMM analysis of thin-wire grids

Sena Esen BAYER KESKİN^{1,*}, Ahmet Arif ERGİN²

¹Mechatronics Engineering Department, Kocaeli University, Kocaeli, Turkey

²Electronics Engineering Department, Gebze Institute of Technology, Kocaeli, Turkey

Received: 05.09.2012 • Accepted: 17.12.2012 • Published Online: 21.03.2014 • Printed: 18.04.2014

Abstract: This article presents a new approach for the analysis of electromagnetic scattering from a rectangular wire mesh. In this sense, a basis function that considers the flow of a current from one cell to the next is proposed in light of Floquet's theorem. The proposed basis function enables the use of periodic method of moments in frequency-selective surfaces composed of thin wires in the case of a system having a connection with neighboring cells, such as thin-wire grids. The validity of the proposed solution approach is tested in 2 distinct cases (with and without a neighbor connection) for scattered fields. It is found that the results of the numerical analyses conducted with the proposed approach are in good agreement with the experimental data. Although the study presented herein focuses only on wire structures, the idea can also easily be extended to surface basis functions.

Key words: Frequency-selective surface, periodic method of moments, reflection/transmission coefficients, thin wires

1. Introduction

The scattering from a frequency-selective surface (FSS) has been the subject of numerous studies [1–13]. In these studies, solutions of electromagnetic wave scattering from periodic arrays of patches or apertures were performed by the variational approach [1], conjugate gradient method [7–10], spectral-iteration approach method [4], method of moments (MoM) [2,5,6,11], and periodic method of moments (PMM) [12,13]. Most of these studies solve the operator equations for the induced surface current density or the aperture field [1–9], which are related by Babinet's principle [3] for flat scatterers. This alleviates the need for modeling unknown currents or fields that continue on to the neighboring cells, since one can choose the entity (current or field) that does not cross the cell edges as the unknown. To determine the scattering characteristics from a wire mesh structure, the 'equivalent radius' concept, in which an equivalence between wires and strips, as described in [14], is used to model the actual round wire as a flat strip, was employed [10,11]. Hence, the wire mesh problem has been turned into a flat surface type problem, which can be formulated for the current density or the aperture field as desired. Alternatively, Blackburn and Arnaut [13] used a PMM with thin-wire kernel for modeling scattering from FSSs made up of wires. However, the approach followed in [13] did not consider FSSs with wire connections between neighboring cells, such as wire mesh structures. In the case of FSSs that have wire connections between neighboring cells, the current flowing from one cell to the next one (i.e. cross-cell currents) needs to be described consistently. However, such a necessity has not been openly addressed in previous studies. In [11], special attention was given to ensure the vector continuity of the current at wire junctions within a cell,

*Correspondence: senabayer@kocaeli.edu.tr

and examples that should involve cross-cell currents are presented. However, no discussion on how the vector continuity of cross-cell currents was explained, even in [11]. In this paper, a simple approach to handle cross-cell currents is presented in light of Floquet's theorem [15], by which the currents in adjacent cells are related to each other by a phase factor, as shown in the next section. Hence, an example of a FSS composed of z directed dipoles is shown in Figure 1, where the currents at points 1 and 2 in Figure 1a must have the same magnitude with a phase shift. It is shown that this can be achieved using a single basis function across neighboring cells.

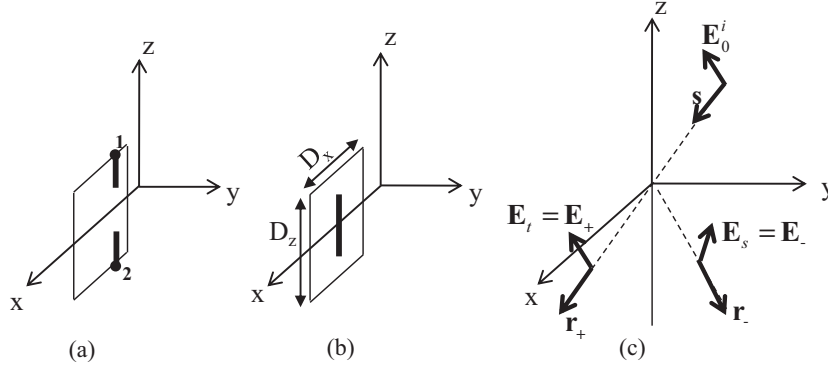


Figure 1. a) Unit cell for configuration 1, b) unit cell for configuration 2, and c) definitions of the vectors used.

In the following sections, first, the concept of PMM formulation is outlined briefly and the incorporation of the cross-cell currents is explained. Next, the measurement setup used for the validation measurements is described. Finally, the effectiveness of the proposed approach is presented in the validation and numerical results section.

2. Formulation

Let us consider a single-layer planar periodic surface of infinite extent that is periodic in the $x - z$ plane with periods denoted by D_x and D_z in the x and z directions, respectively. Within each unit cell, there is an arbitrary shaped wire that lies entirely within the plane of the mesh. The mesh is illuminated by a monochromatic plane wave, which is represented by $\mathbf{E}^i = \mathbf{E}_0^i \exp(-j\beta \mathbf{R} \cdot \mathbf{s})$, with linear polarization and an arbitrary direction of propagation denoted by the unit vector $\mathbf{s} = \hat{x}s_x + \hat{y}s_y + \hat{z}s_z$. Here, \mathbf{R} is an arbitrary observation point in space and $\beta = 2\pi/\lambda$ is the propagation constant in free space. PMM is used to determine the currents on this wire structure, such that the tangential component of the electric field vanishes on the wire surfaces [13].

The element currents are all related to each other by Floquet's theorem [15]:

$$I_{qm}(l) = I_{00}(l) \exp(-j\beta q D_x s_x) \exp(-j\beta m D_z s_z), \quad (1)$$

where $I_{00}(l)$ represents the current over the reference element $(0,0)$, while I_{qm} stands for the current flowing in the unit cell with index (q, m) at point l along the wire. Since the element currents are periodic across unit cells according to Floquet's theorem, only a reference current element needs to be calculated. The total field \mathbf{E} can be obtained by superposition over all cells. The total scattered field on the transmission side (denoted by '+') and the reflection side (denoted by 't') can be expressed using Poisson's sum rule to transform the

summation to the spectral domain as [12]:

$$\mathbf{E}_{\pm}(\mathbf{R}) = \int_0^L \frac{Z}{2D_x D_z} I(l) \times \sum_{n_x, n_z} \frac{1}{r_y} \exp\{-j\beta[\mathbf{R} - \mathbf{R}(l)] \cdot \mathbf{r}_{\pm}\} \mathbf{e}_{\pm}(l) dl. \quad (2)$$

In Eq. (2), $\mathbf{R}(l)$ is a reference point on the reference element, Z is the free-space impedance, $I(l)$ is the local current in the wire, L is the wire length, \mathbf{r}_{\pm} is the direction of propagation, $\mathbf{e}_{\pm}(l) = [\hat{\mathbf{p}}(l) \times \mathbf{r}_{\pm}] \times \mathbf{r}_{\pm}$ is the polarization vector, and $\hat{\mathbf{p}}(l)$ is the local unit vector in the direction of the wire axis. For interested readers, detailed information related to the PMM can be found in [13].

For wire mesh FSSs, triangular basis functions are used for expanding the unknown currents [13]. The usual triangular basis function, which is related to the consecutive nodes $\{l_{n-1}, l_n, l_{n+1}\}$, is defined as:

$$T_n(l) = \begin{cases} 1 - (l_n - l)/(l_n - l_{n-1}) & ; l_{n-1} < l < l_n \\ 1 - (l - l_n)/(l_{n+1} - l_n) & ; l_n < l < l_{n+1} \end{cases}. \quad (3)$$

However, this basis function is not sufficient to describe the cross-cell currents. Therefore, we introduce the cross-cell triangular basis function related to the nodes $\{l_{n-1}, l_n; l_{n+1}, l_{n+2}\}$, assuming that the nodes $\{l_n, l_{n+1}\}$ denote the same cross-cell point. Combining Eq. (3) with Eq. (1), the cross-cell basis can be expressed as:

$$T_n(l) = \begin{cases} 1 - (l_n - l)/(l_n - l_{n-1}) & ; l_{n-1} < l < l_n \\ [1 - (l - l_n)/(l_{n+1} - l_n)] e^{-j\beta q D_x s_x} e^{-j\beta m D_z s_z} & ; l_{n+1} < l < l_{n+2} \end{cases}, \quad (4)$$

where $(q, m) \in \{-1, 0, 1\}$. If the basis function lies along the z direction, $m \in \{-1, 1\}$ and $q = 0$; otherwise, $q \in \{-1, 1\}$ and $m = 0$.

Solving Eq. (2) using the PMM, the reflection coefficient can be found as:

$$Rc = 20 \log \left(\frac{\mathbf{E}_s}{\mathbf{E}_i} \right), \quad (5)$$

and the transmission coefficient can be found as:

$$Tc = \frac{\mathbf{E}_t + \mathbf{E}_i}{\mathbf{E}_i}. \quad (6)$$

Here, $\mathbf{E}_s = \mathbf{E}_-$ is the scattered field, $\mathbf{E}_t = \mathbf{E}_+$ is the transmitted field, and \mathbf{E}_i stands for the incident field.

3. Validation and numerical results

The efficacy of using the suggested basis functions, which allow currents to flow between neighboring cells, will be demonstrated in this section. The first example is chosen as an FSS composed of z directed dipoles that form a simple structure. Next, scattering from a wire mesh is presented together with the measurement results as the second example.

3.1. Dipole FSS

In the first example, a FSS composed of z directed dipoles, as seen in Figure 1, is used. Two discretization configurations are used, as in Figures 1a and 1b and the vector definitions given in Figure 1c. Due to their

simple geometry and ease of computation, dipole arrays are chosen to show that choosing the usual triangle basis or the cross-cell basis functions does not affect the result. In the example studied here, $D_x = D_z = 6$ mm, the dipole length is 4 mm, and the radius is $50 \mu\text{m}$. The dipole has 8 segments and each segment has a length of 0.5 mm. In configuration 2 (Figure 1b), each dipole is well confined to a unit cell. On the other hand, in configuration 1 (Figure 1a), the FSS unit cell is chosen so that the system allows a current flow between the cells. Since both configurations describe the same FSS, it is expected to obtain the same results from their solutions. Reflection coefficients are calculated for normal incidence and \mathbf{z} polarized \mathbf{E}_i using the PMM and are compared for configurations 1 and 2 in Figure 2. The results are in perfect agreement.

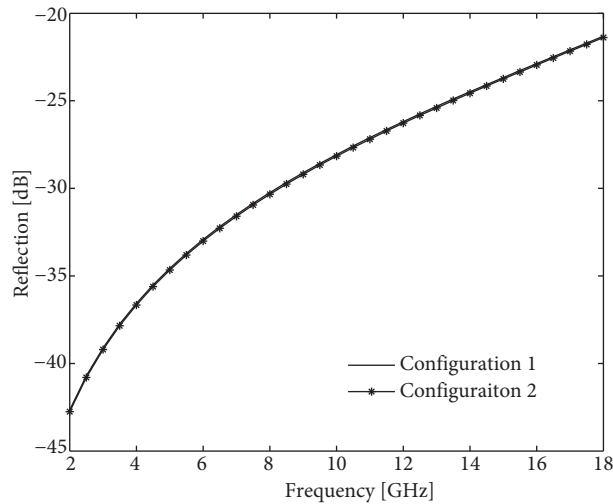


Figure 2. Reflection coefficient for configurations 1 and 2.

3.2. Wire-grid FSS

As a second example, a wire-grid FSS is considered. Each cell has wires in a cross arrangement and there are wire connections between the cells. The unit cell structure is given in Figure 3. Here, $D_x = D_z = 3.75$ mm and the discretization has a segment length of 0.375 mm. The wire diameter is $140 \mu\text{m}$. The basis function given in Eq. (3) is used to model the currents flowing from node 16 to node 17 and from node 6 to node 7 (see Figure 3). Using the PMM, reflection and transmission coefficients are calculated for normal incidence and for both horizontal/horizontal (HH) and vertical/vertical (VV) polarizations. A wire mesh with the same properties is constructed and the reflection and transmission coefficients are measured. The measurement setup is given in Figure 4 [16]. The dimensions of the main chamber of the measurement system are $240 \times 120 \times 120$ cm and it includes 2 identical sections separated by a sliding window, which is made of aluminum and has an aperture of 40×40 cm to insert the sample. Both parts of the chamber (including the doors) are electromagnetic interference-isolated, and the inner walls are covered with microwave pyramid absorbers. When an aluminum sheet is placed as the sample, the isolation between the 2 chambers is measured to be in excess of $t40$ dB throughout the 2 to 18-GHz operation band. The transmit and receive antennas are Satimo-type SH-2000 dual-ridge horn antennas. The antennas can be rotated so that all 4 polarization-type measurements can be carried out. The numerical results are compared with the measurements in Figure 5 for both the reflection and the transmission coefficients. Figure 5 shows that the numerical results for the VV and HH polarizations are the same as expected, since the dimensions of the grid are the same in both the x and z directions. For the reflection coefficients, the difference between the numerical and experimental results is less than 0.1, which is

determined to be the accuracy limit of the measurement system. The excessive errors, which have a saw-tooth pattern, in the frequency range of 2–3 GHz, are known to emerge due to the measurement system itself. For the transmission coefficients, the measurement system is more stable and the results of the measurement and computations agree well in the whole frequency range of 2–18 GHz for both the VV and HH polarizations. In Figure 6, the variation of the reflection and transmission coefficients as a function of the wire diameter is studied. The reflectivity shows a direct proportion with the diameter and the transmittivity shows an inverse proportion with the diameter.

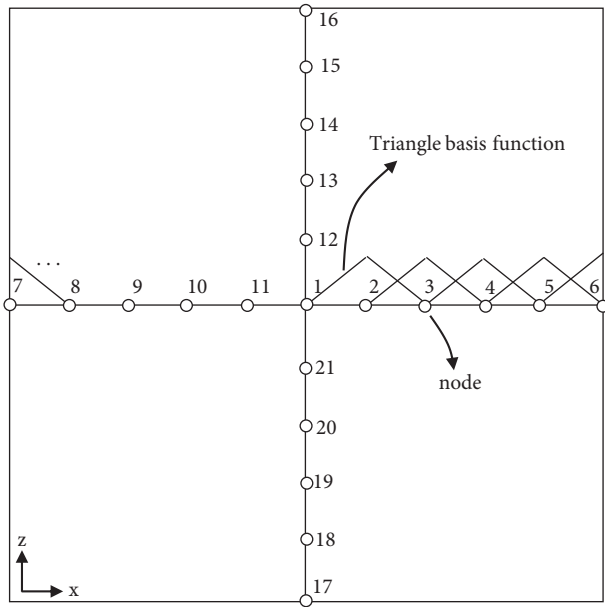


Figure 3. Unit cell of the wire-grid FSS.

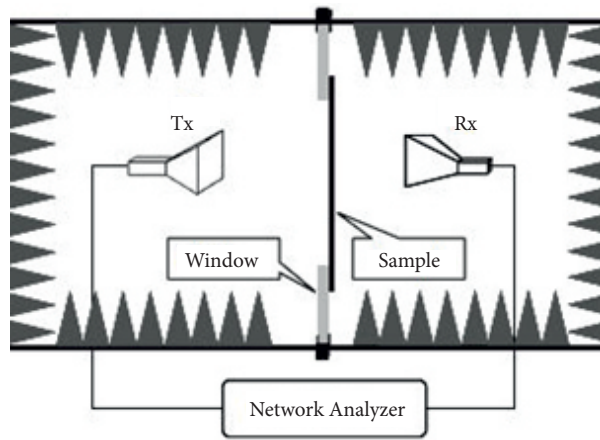


Figure 4. Measurement system.

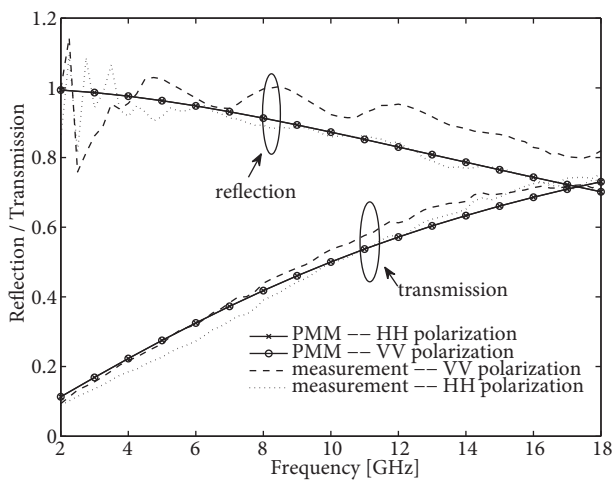


Figure 5. Reflection/transmission coefficients for the mesh structure.

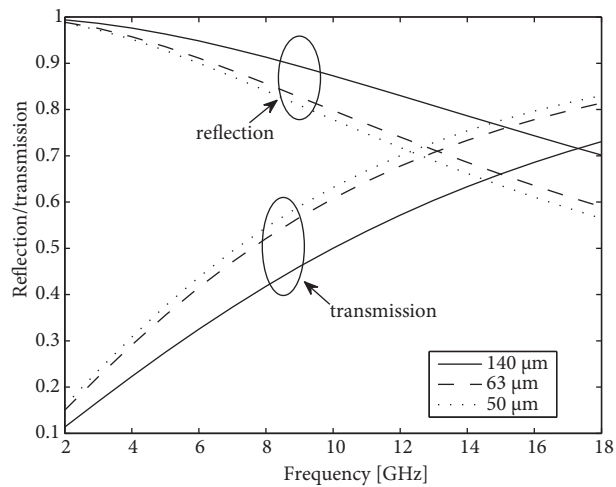


Figure 6. Reflection/transmission coefficients for different wire diameters (PMM results).

4. Conclusion

A new method to modify the basis functions in the PMM analysis of periodic structures that enable the representation of the currents flowing from one cell to the next is introduced and validated. It is shown that the introduced basis functions perform well based on numerical examples and comparisons with measurements.

References

- [1] R. Kiebertz, A. Ishimaru, "Aperture fields of an array of rectangular apertures", *IRE Transactions on Antennas and Propagation*, Vol. 10, pp. 663–671, 1962.
- [2] C.C. Chen, "Transmission through a conducting screen perforated periodically with apertures", *IEEE Transactions on Microwave Theory and Techniques*, Vol. 18, pp. 627–632, 1970.
- [3] C.C. Chen, "Scattering by a two-dimensional periodic array of conducting plates", *IEEE Transactions on Antennas and Propagation*, Vol. 18, pp. 660–665, 1970.
- [4] C.H. Tsao, R. Mittra, "A spectral-iteration approach for analyzing scattering from frequency selective surfaces", *IEEE Transactions on Antennas and Propagation*, Vol. 30, pp. 303–308, 1982.
- [5] T. Cwik, R. Mittra, K. Lang, T. Wu, "Frequency selective screens", *IEEE Antennas and Propagation Society Newsletter*, Vol. 29, pp. 5–10, 1987.
- [6] R. Mittra, C.H. Chan, T. Cwik, "Techniques for analyzing frequency selective surfaces-a review", *Proceedings of the IEEE*, Vol. 76, pp. 1593–1615, 1988.
- [7] C.H. Chan, R. Mittra, "On the analysis of frequency-selective surfaces using subdomain basis functions", *IEEE Transactions on Antennas and Propagation*, Vol. 38, pp. 40–50, 1990.
- [8] T. Cwik, R. Mittra, "Scattering from a periodic array of free-standing arbitrarily shaped perfectly conducting or resistive patches", *IEEE Transactions on Antennas and Propagation*, Vol. 35, pp. 1226–1234, 1987.
- [9] J.P. Montgomery, K.R. Davey, "The solution of planar periodic structures using iterative methods", *Electromagnetics*, Vol. 5, pp. 209–235, 1985.
- [10] C. Christodoulou, J. Kauffman, "On the electromagnetic scattering from infinite rectangular grids with finite conductivity", *IEEE Transactions on Antennas and Propagation*, Vol. 34, pp. 144–154, 1986.
- [11] W.A. Imbriale, V. Galindo-Israel, Y. Rahmat-Samii, "On the reflectivity of complex mesh surfaces [spacecraft reflector antennas]", *IEEE Transactions on Antennas and Propagation*, Vol. 39, pp. 1352–1365, 1991.
- [12] B. Munk, *Frequency selective surfaces: Theory and design*, New York, Wiley, 2000.
- [13] J. Blackburn, L.R. Arnaut, "Numerical convergence in periodic method of moments analysis of frequency-selective surfaces based on wire elements", *IEEE Transactions on Antennas Propagation*, Vol. 53, pp. 3308–3315, 2005.
- [14] C. Butler, "The equivalent radius of a narrow conducting strip", *IEEE Transactions on Antennas and Propagation*, Vol. 30, pp. 755–758, 1982.
- [15] M.G. Floquet, "Sur les equations differentielles lineaires a coefficients periodiques", *Annale Ecole Normale Superieur*, pp. 47–88, 1883.
- [16] S.E. Bayer, A. Çelik, A.A. Ergin, "Reflection/transmission measurement system for planar materials and verification by thin wire grids", *The 30th General Assembly and Scientific Symposium of the International Union of Radio Science*, 2011.